International Journal of Cardiology 174 (2014) 25–30

Contents lists available at ScienceDirect

International Journal of Cardiology

journal homepage: www.elsevier.com/locate/ijcard

Aortic coarctation and the retinal microvasculature☆,☆☆

Laurianne Le Gloan [a], Hadi Chakor [a], Lise-Andrée Mercier [a], Paul Harasymowycz [c], Annie Dore [a], Pierre Lachapelle [d], Josephine Pressacco [b], Bernard Thibault [a], François Marcotte [a], Anna Proietti [a], Hugues Leduc [e], Blandine Mondésert [a], François-Pierre Mongeon [a], Jean-Claude Tardif [a,e], Paul Khairy [a,e,*]

[a] Department of Medicine, Montreal Heart Institute, Université de Montréal, Montreal, Canada
[b] Department of Radiology, Montreal Heart Institute, Université de Montréal, Montreal, Canada
[c] Department of Ophthalmology, Hôpital Maisonneuve-Rosemont, Université de Montréal, Montreal, Canada
[d] Department of Ophthalmology, Montreal Children's Hospital Research Institute, McGill University, Montreal, Canada
[e] Montreal Health Innovations Coordinating Center (MHICC), Université de Montréal, Montreal, Canada

ARTICLE INFO

Article history:
Received 7 February 2014
Accepted 14 March 2014
Available online 21 March 2014

Keywords:
Aortic coarctation
Hypertension
Retinal vessels
Cardiovascular risk factors

ABSTRACT

Background: Aortic coarctation has been associated with generalized vascular disease, yet little is known about retinal vascular patterns and their changes over time.

Objectives: The aim of this study is to characterize the nature and extent of retinal vascular disease in adults with aortic coarctation, and explore age-related effects and associations with cardiovascular outcomes.

Methods: A prospective cross-sectional seroepidemiological study was conducted on 60 consecutive adults with repaired aortic coarctation, age 42.4 ± 14.1 years, 61.7% male. In addition to detailed questionnaires, imaging studies, and laboratory testing, high-quality retinal images were acquired by 45° nonmydriatic digital funduscopy.

Results: No patient had evidence of hypertensive retinopathy. A distinctive vascular pattern characterized by bilaterally symmetric tortuosity of retinal arteries and veins was observed. Arterial tortuosity was abnormal in 98.3% of patients and decreased with age ($P = 0.0005$). In patients ≥45 years, a 1-point increase in the arterial tortuosity score was associated with a 1.5-fold higher risk of cardiovascular complications (i.e., acute coronary syndrome, stroke, cerebral aneurysm, aortic dissection/rupture) [odds ratio 1.50, 95% CI (1.01, 2.24), $P = 0.0496$]. Abnormal venous tortuosity was present in 75.0% of patients and non-significantly correlated with higher levels of serum inflammatory markers (C-reactive protein, fibrinogen, interleukin-6, and tumor necrosis factor-alpha). A higher venous tortuosity score was likewise associated with an increased risk of cardiovascular complications [odds ratio 1.86, 95% CI (1.03, 3.35), $P = 0.0392$].

Conclusions: Adults with repaired aortic coarctation exhibit a unique retinal vascular pattern characterized by excessive arterial and venous tortuosity that regresses with age. Greater tortuosity is associated with adverse cardiovascular outcomes in patients ≥45 years.

1. Introduction

Aortic coarctation is a common congenital defect characterized by narrowing of the aortic arch, typically near the insertion site of the ductus arteriosus [1]. Despite advances in percutaneous interventions, surgical repair, and medical therapies, long-term prognosis is marred by morbidity and excess mortality related to vascular complications such as systemic arterial hypertension, accelerated coronary atherosclerosis, aortic dissection and rupture, and cerebrovascular accidents [2–4]. Although the pathogenesis remains poorly understood, intrinsic vascular abnormalities have been hypothesized to contribute to these late-onset adverse outcomes that cannot be reliably predicted by standard factors, such as severity of the initial obstruction or type of repair.

The ocular fundus is the only location in the body where blood vessels can be visualized. In other patient populations, retinal vascular changes have been associated with acute coronary syndromes, stroke, systemic biomarkers of endothelial function, and cardiovascular mortality, independent of traditional cardiovascular risk factors [5–7]. Despite concerns expressed as early as 1948 about retinal vascular abnormalities in patients with aortic coarctation [8,9], few studies

Abbreviations: A/V, Arteriovenous; CAIAR, Computer Assisted Image Analysis of the Retina; CRAE, Central retinal artery equivalent; CRVE, Central retinal vein equivalent; MRI, Magnetic resonance imaging; SIVA, Singapore "I" Vessel Assessment.

☆ Financial support: The study was supported by a Canada Research Chair in Electrophysiology and Adult Congenital Heart Disease (PK) and the Montreal Heart Institute Foundation.

☆☆ Relationships with industry: JCT holds the Université de Montréal Pfizer-endowed research chair in atherosclerosis and the Canada Research Chair in translational and personalized medicine.

* Corresponding author at: Montreal Heart Institute Adult Congenital Center, 5000 Bélanger E., Montreal, Quebec, Canada, H1T 1C8. Tel.: +1 514 376 3330x3652; fax: +1 514 593 2581.

E-mail address: paul.khairy@umontreal.ca (P. Khairy).

http://dx.doi.org/10.1016/j.ijcard.2014.03.129
0167-5273/

have commented on fundoscopic findings [10] and none have explored correlations with cardiovascular events. Leveraging advances in digital fundoscopic technology, we sought to characterize retinal microvascular patterns in adults with repaired aortic coarctation, quantify the prevalence and extent of retinal vascular changes, and explore associations with age and adverse cardiovascular outcomes.

2. Material and methods

2.1. Study population

A total of 60 adults (≥18 years of age) with repaired aortic coarctation were prospectively enrolled from the Montreal Heart Institute Adult Congenital Centre between June 2010 and December 2012. Patients with Turner syndrome, contraindications to magnetic resonance imaging (MRI), or concomitant forms of congenital heart disease (other than bicuspid aortic valve and repaired simple shunt lesions) were excluded. The study protocol was approved by the Montreal Heart Institute Review Board and all participants provided written informed consent.

2.2. Study design and clinical assessment

A prospective cross-sectional seroepidemiological study was conducted consisting of a baseline questionnaire, physical examination, two-dimensional and M-mode Doppler echocardiography, laboratory testing, cerebral MRI, and bilateral digital fundoscopy.

The clinical assessment included demographic variables, height, weight, body mass index, associated defects (i.e., bicuspid aortic valve or shunt lesion), surgical and interventional history, cardiovascular risk factors [i.e., systemic arterial hypertension, hypercholesterolemia, diabetes mellitus, family history of cardiovascular disease (first degree male relative under 55 years or female relative under 65 years), and current cigarette smoking], pharmacological therapies, comorbidities, and cardiac and cerebrovascular disease (e.g., acute coronary syndromes, established coronary artery disease, stroke, transient ischemic attack, aortic dissection or rupture, and previously diagnosed cerebral aneurysms). Blood pressure was obtained by averaging three consecutive measurements at 5-min intervals separately in the right arm and right leg [11].

Echocardiographic assessment included left ventricular mass, aortic root dimensions at various levels (i.e., aortic annulus, sinuses of Valsalva, sinotubular junction, and proximal ascending aorta) and residual gradient at the site of the aortic isthmus. Due to cost constraints, cardiac MRI was performed if deemed clinically indicated, with aortic dimensions retained for analyses. Magnetic resonance angiography of the intracranial arteries was conducted using a 1.5-Tesla scanner (Philips, Netherlands) with source data reviewed in three orthogonal planes (field of view 200 mm; field of view phase 75; section thickness 0.83 mm). Post processing maximum intensity projection images were generated for multiplanar reformatting.

A single venous blood sample was drawn. After centrifugation at 3500 rpm at 4 °C for 15 min, samples were collected and stored at −80 °C until assayed. Standard methods were used to quantify serum concentrations of potassium, creatinine, lipids [i.e., total cholesterol, low- (LDL) and high-density (HDL) lipoproteins, and triglycerides], high-sensitivity C-reactive protein (CRP), and plasma fibrinogen levels. Serum levels of interleukin-6 (IL-6) and tumor necrosis factor-alpha (TNF-alpha) were determined by enzyme-linked immunosorbent assays (R&D systems, Germany).

2.3. Ophthalmic evaluation

The ophthalmology team charged with obtaining, processing, and interpreting digital retinal images was blinded to the patient's clinical history. After 5 min of dark adaptation, a 45° funduscopic examination was performed to acquire high-quality images using a Canon 9 megapixel non-mydriatic digital camera (CR-DGI 40D, Canon USA, Melville, NY) with a retinal vessel analysis software (Singapore "I" Vessel Assessment, version 1.0, 2010) [12]. The exam, which lasted approximately 15 min, was performed in a sitting position with the patient's chin on a chin rest and forehead pressed against a headrest. Patients were asked to focus on a fixation target. Detailed images of the macula and posterior pole vessels were obtained. Pictures were taken simultaneously on right and left eyes and centered on optic disks.

As illustrated in Fig. 1, all vessel segments coursing through the area between one and two times the optic disk diameter, extending from its outer boundary, were traced and identified as arteries or veins. Bilateral central retinal artery and vein diameters were measured semi-automatically by means of the SIVA program, from which the mean arterio-venous (A/V) ratio was calculated. Tortuosity of retinal arteries and veins, defined as the integral of the curvature square along the vessel path normalized by path length, was quantified by a previously described semi-automatic method using the validated Computer Assisted Image Analysis of the Retina (CAIAR) program [13–15]. CAIAR identifies vessel segments (typically 10 to 16 per eye) and determines tortuosity measurements for each segment beyond a 120-pixel diameter circle centered on the optic disc (to exclude overlapping vessels emerging from the disc) to a diameter of 400 pixels (equivalent to an area of 100 mm^2). Average measurements were summarized as a tortuosity score separately for arteries and veins. Units of tortuosity represent a ratio and are, therefore, continuous and dimensionless [14].

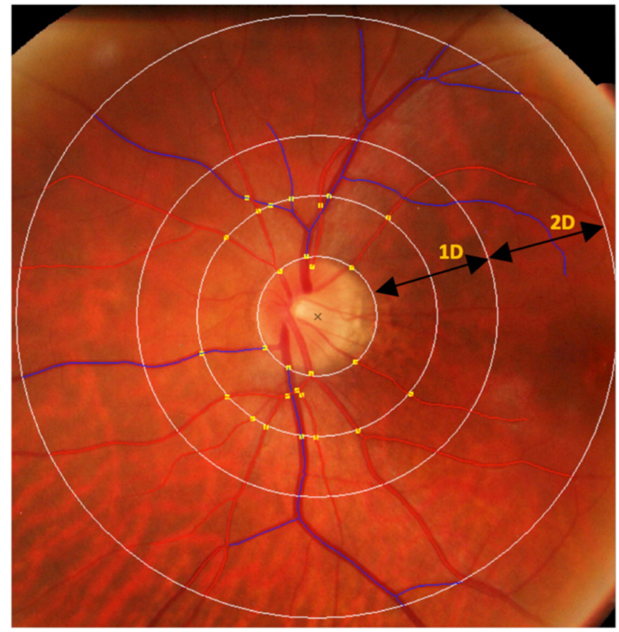

Fig. 1. Retinal vessel calibre and tortuosity scores. Shown is a 45° fundus retinal image centered on the optic disk. For illustrative purposes, retinal arteries are indicated in red and veins in blue. Retinal vessel calibres and tortuosity scores were measured semi-automatically for all vessel segments coursing through the area between one (1D) and two (2D) times the diameter of the optic disk.

2.4. Statistical analysis

Continuous variables are summarized by mean ± standard deviation or median and interquartile range (IQR; 25th, 75th percentile), depending on their distribution. Categorical variables are represented by frequencies and percentages. Baseline variables according to severity of retinal arterial tortuosity, classified as normal (≤5) or mild (>5 and ≤7), moderate (>7 and ≤9), and severe (>9), were compared by nonparametric Kruskal Wallis, chi-square, or Fisher Exact tests, where appropriate (Table 1). Prevalence values and their 95% confidence intervals (CI) were estimated for abnormal arterial and venous tortuosity scores and A/V ratio. Factors associated with arterial (Table 2) and venous (Table 3) tortuosity scores and the A/V ratio (Table 4) were explored in univariate and multivariate linear regression models. Variables associated with *P*-values <0.2 in univariate analyses were entered into automated stepwise multivariate regression models. Factors associated with adverse cardiovascular outcomes (i.e., acute coronary syndrome, stroke, transient ischemic attack, cerebral aneurysm, aortic dissection or rupture) were explored in logistic regression analyses that included first-order interaction terms between age and tortuosity scores. Two-tailed *P*-values <0.05 were considered statistically significant. Statistical analyses were performed using SAS software, version 9.3 (SAS Institute, Cary, NC).

3. Results

3.1. Baseline characteristics

A total of 60 patients, age 42.4 ± 14.1 years, 61.7% male were prospectively enrolled. Baseline characteristics are summarized in Table 1. The aortic valve was bicuspid in 27 (45.0%) patients. Aortic coarctation repair was performed at a median age of 8.4 (IQR 4.3, 20.8) years. Fourteen (23.3%) patients had primary balloon dilation and/or stenting, whereas 46 (76.7%) had surgical repair consisting of a termino-terminal anastomosis in 30 (50.0%), subclavian flap in 9 (15.0%), and patch aortoplasty or bypass graft in 7 (11.7%). Cardiovascular risk factors included hypercholesterolemia in 13 (21.7%) patients, hypertension in 28 (46.7%), diabetes in 1 (1.7%), family history of premature coronary artery disease in 10 (16.7%), and active cigarette smoking in 9 (15.0%).

3.2. Retinal vessel dimensions and the A/V ratio

Nonmydriatic fundoscopic high-quality digital retinal images were successfully acquired in all patients. No patient had evidence of a retinal